Sinuous breakdown in a flat plate boundary layer exposed to free-stream turbulence

Sinuous breakdown in a flat plate boundary layer exposed to free-stream turbulence

J. Mans, H. C. de Lange,[a] and A. A. van Steenhoven
Laboratory for Energy Technology, Department of Mechanical Engineering, Eindhoven University of Technology, P.O. Box 513, 5600 MB Eindhoven, The Netherlands

(Received 13 April 2007; accepted 24 May 2007; published online 14 August 2007)

In a flat plate boundary layer, perturbed with streaks, breakdown occurs due to a secondary instability acting on the streaks. An experimental study using a water channel with static turbulence grid revealed the presence of a sinuous secondary instability mode in the bypass transition process. Five sinuous instabilities are investigated in detail in the horizontal plane. The streamwise length scale of the sinuous instability is around $40\delta^*_{300}$ and the spanwise scale equals around δ^*_{300}. Four main features are found in the underlying streak configuration and developing streak-streak interactions. Firstly, all instabilities arise in a streak configuration where two low-speed streaks are located at a small spanwise distance from each other. Patches of low-speed fluid (forming a discontinuity in the streak pattern) are present in the high-speed streaks surrounding the unstable low-speed streak. As a consequence of the streak-streak interactions at the discontinuities, vortices arise in a staggered configuration. Finally, the vortices develop into three-dimensional structures after which the flow falls apart into smaller three-dimensional flow regions. © *2007 American Institute of Physics*. [DOI: 10.1063/1.2750684]

A flat plate boundary layer flow exposed to free-stream turbulence is characterized by the presence of long elongated structures with alternating low and high streamwise velocity in the boundary layer. The existence of these streaks has been experimentally confirmed in the studies by Kline.[1] The streaks appear already in the first stages of the boundary layer and are highly stable. The streaks evolve in the downstream direction and at a certain point they breakdown into turbulence, which results in a turbulent spot.[2]

The visualization results of Matsubara and Alfredsson[3] in a flat plate boundary layer showed that just before breakdown the streaks undergo a streamwise waviness of relatively short wavelength. This oscillation develops further into a turbulent spot. Brandt *et al.*[4] and Jacobs and Durbin[5] performed numerical simulations of a boundary layer exposed to free-stream turbulence. In these numerical studies the authors are able to retrieve the instabilities initiating a turbulent spot. This made it possible to study the natural, unforced, breakdown process. Both studies report that natural spot precursors are localized instabilities of single low-speed streaks. Brandt *et al.*[4] present flow structures of typical spot precursors that can be classified as sinuous (antisymmetric oscillation in spanwise direction) and varicose (symmetric oscillation in spanwise direction) instabilities. It is concluded that the breakdown is related to local instabilities driven by the strong shear layers between the alternating streaks. The sinuous secondary instability is driven by the spanwise shear and the varicose instability by wall-normal shear. In the opposite, Jacobs and Durbin[5] and Durbin and Wu[6] conclude that turbulent spot precursors consist of low-speed streaks extending into the upper portion of the boundary layer, where they interact with free-stream eddies and then develop into a patch of irregular motion. The irregular motion can neither be ascribed to a sinuous nor a varicose motion of the streak pattern. Schoppa and Hussain[7] report a streak transient growth mechanism present in a channel flow in which spanwise perturbations undergo a strong transient growth resulting in a sheet of streamwise vorticity, after which a sinuous streak waviness starts to grow. Recent results of Hoepffner *et al.*[8] on the transient growth of secondary instabilities indicate that, for a boundary layer flow, the optimal initial condition undergoing secondary transient growth consists of velocity perturbations (closely resembling the unstable eigenfunctions obtained for streaks of higher amplitudes) localized in the regions of highest shear of the streak base flow. The spanwise velocity component of the optimal sinuous perturbation is the dominant one, which explains the transient growth of the pure spanwise perturbation from Schoppa and Hussain.[7]

In this Communication the natural (no additional triggering is used) breakdown process induced by a sinuous secondary instability in a flat plate boundary layer perturbed with streaks is experimentally examined in the horizontal $x-z$ plane. The primary objectives of this research are to provide careful experiments that can identify the streamwise and spanwise length scales of the natural sinuous secondary instability as well as the underlying streak configuration and characteristic streak-streak interactions occurring during the development of the instability. The provided data can be used for comparison with theory and/or numerical simulations. The results provide, according to the authors, for the first time, detailed experimental information on the natural sinuous secondary instability of low-speed streaks.

The natural sinuous instability is experimentally investigated in a water channel (Mans *et al.*[9]) in the horizontal

[a]Author to whom correspondence should be addressed. Telephone: +31 40 247 2129. Electronic mail: h.c.d.lange@tue.nl

TABLE I. Streamwise range of the five sinuous instabilities.

Event	Streamwise range		Sequence length	$\Delta t^* = \Delta t U_\infty / \delta^*_{300}$	Symbol
	Re_{xstart}	Re_{xend}			
Instability 1	1.39×10^5	1.63×10^5	31	109	○
Instability 2	1.73×10^5	1.98×10^5	33	116	*
Instability 3	0.49×10^5	0.71×10^5	30	106	
Instability 4	0.39×10^5	0.59×10^5	27	95	◇
Instability 5	1.17×10^5	1.41×10^5	33	116	×

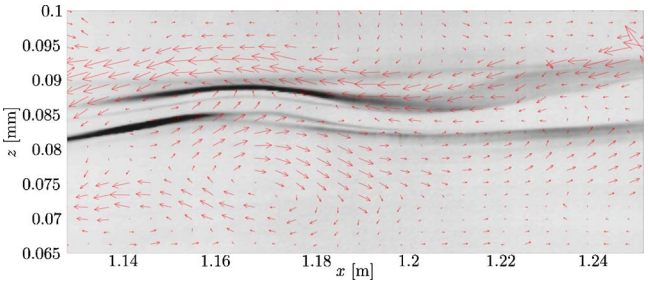

FIG. 1. (Color online) A typical combined PIV-LIF result, $U_\infty = 0.125$ m/s and $1.52\times10^5 < Re_x < 1.56\times10^5$. The vector plot presents the disturbance field (u', w') while the gray scale indicates the dye intensity.

$x-z$ plane, 5 mm above the flat plate using a combined (particle image velocimetry) PIV and dye visualization measurement technique.[10] The evolution of the flow structures during the bypass transition process is observed while moving along with the flow with a velocity of 0.09 m/s in the downstream direction, enabled by a camera traversing system. This velocity equals the average velocity of flow structures at the measurement height. The output of one experimental run consists of the visualizations of the dye streak lines and the corresponding instantaneous velocity fields. The "typical" sinuous motion of the unstable streak in the dye visualizations[9] are used to identify the velocity fields in which a sinuous instability develops. The calculation of the velocity fields is carried out by means of the software package PIVtec.

Streaks are generated by exposing the experimental boundary layer to grid-generated free-stream turbulence. The free-stream turbulence characteristics above the leading edge of the plate are[11] turbulence intensity, Tu=5.8%, $u'/\nu = 5\times10^3$ m^{-1}, integral length scale $Re_L = 125$, Taylor scale $Re_\lambda = 25$, and Kolmogorov scale $Re_\eta = 3.5$. A characteristic value of the boundary layer thickness is $\delta^*_{300} = 2.4$ mm, where δ^*_{300} is a scaling parameter defined as $Re_{\delta^*_{300}} = 300$, where $Re_{\delta^*_{300}} = U_\infty \delta^*_{300}/\nu$.

Out of 2000 measurement runs, 5 could be selected in which a developing unstable low-speed streak shows a sinuous wavy motion. Due to the random character of the natural breakdown process and the subsequent spot appearance, a stable (laminar) boundary layer is present in the recording domain of the other measurement runs. The five selected runs show a breakdown pattern within the field of view. Table I presents for each instability Re_{xstart}, which corresponds to the Reynolds number based on the center of the first instantaneous velocity field in which the disturbance field shows the beginning of a sinuous oscillation. Re_{xend} corresponds to the Reynolds number of the disturbance field in which the flow starts to fall apart into smaller three-dimensional flow regions. The table also displays the dimensionless time lapse, Δt^*, in which each instability develops, using U_∞ and δ^*_{300}. The last column presents the symbols used in the following to distinguish the different cases. The table shows that the sinuous instability starts at the average position $Re_x = 1.02\times10^5$, and at $Re_x = 1.26\times10^5$, after a time lapse of 108, the unstable streaks fall apart into smaller three-dimensional flow regions. The variance in the specific values of the five instabilities in Table I reveals that each instability develops in approximately the same time lapse in spite of the spread in the breakdown position.

A typical image obtained with the combined PIV-visualisation technique, revealing a visualized sinuous instability and the corresponding instantaneous velocity field, is shown in Fig. 1. The figure, presenting instability 1 in Table I, shows an area of 0.12×0.035 m^2 and a corresponding streamwise range of $1.41\times10^5 < Re_x < 1.56\times10^5$. It should be noted that the spanwise axis is stretched by a factor of 1.5 in comparison to the streamwise axis.

The diffusive behavior of the visualization fluid in the downstream part of the images is a result of weak flow phenomena in the upstream streaky flow. The vectors in each image represent the streamwise and spanwise disturbance components, u' and w', respectively, of the instantaneous velocity field (obtained by subtracting the median). The velocity disturbance field shows the present low- and high-speed streaks, which also oscillate in a sinuous way. Furthermore, it is clear that vortices are present in the high shear region in between the high– and low-speed streaks.

The visualization results of Mans *et al.*[9] demonstrate that the sinuous instability is characterized by an antisymmetric oscillation of a low-speed streak and that the amplitude of the oscillation increases spatially as well as in time. The amplitude of the unstable low-speed streak and its development is analyzed in the velocity data. The amplitude and the wavelength of the oscillation are determined at the centerline of the unstable low-speed streak. The points of the streak geometry necessary to calculate the amplitude and wavelength of the oscillation are selected by isolating the geometry of the unstable streak from the remaining of the flow field. The vectors situated in the streak are found by selecting all vectors that satisfy the following velocity criterion:

$$u_{\text{streak}}(x,z) < \alpha \cdot \overline{u_{\text{field}}}, \tag{1}$$

where $\overline{u_{\text{field}}}$ is the mean streamwise displacement of the considered part of the PIV domain and α is a constant. The value of α is chosen in such a way that the selected vector coordinates match the streak profile most optimally.

The amplitude and wavelength development of the oscillation in the velocity fields is analyzed in the sinuous instabilities 1, 2, 4, and 5 from Table I. The third sinuous instability is located too far on the edge of the recording domain to enable a proper analysis. The accuracy of the results is largely governed by the original spatial resolution of PIV data. This spatial resolution is approximately δ^*_{300}. The de-

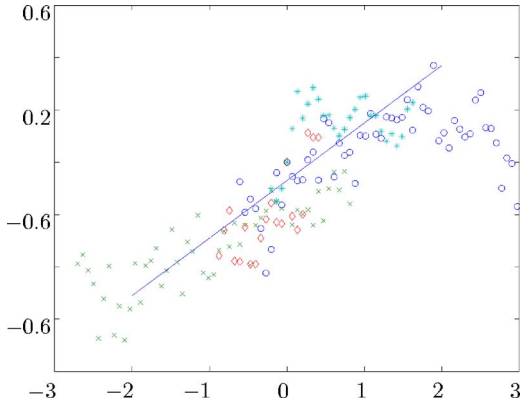

FIG. 2. (Color online) $\ln(A(\chi)/A_0)$; the solid line presents an exponential data fit (symbols defined in Table I).

velopment of the amplitude, A, of the four unstable low-speed streaks is displayed in Fig. 2. Each measurement point in this figure corresponds to an instantaneous moment in time; the same is valid for Fig. 3. The relation between the instabilities and the different symbols is given in the last column of Table I. Figure 2 shows $\ln(A(\chi)/A_0)$, where $\chi=t-t_0$ and A_0 represent the initial value of the amplitude at $t=t_0$. The constant t_0 is chosen such that at $\chi=0$ the amplitude, A, equals δ^*_{300} (which is an arbitrary value).

The amplitude of the sinuous oscillation increases exponentially in the streamwise direction to a maximum value of $\approx 2.1\ \delta^*_{300}$ ($A_0 \simeq 1.3\delta^*_{300}$). The growth rate equals approximately 0.01, made dimensionless with U_∞ and the local boundary layer thickness. This value corresponds well to the growth rate of the sinuous secondary instability found in the direct numerical simulations in Andersson *et al.*[12] When the amplitude of the sinuous oscillation reaches its maximum amplitude value, $A_{\max}$, the oscillation breaks down due to the arising of three-dimensional structures in the disturbance field. This breakdown realizes a deformation of the unstable streak, which results in a decrease of the amplitude.

The spanwise spacing of the streaks, $\overline{\lambda_{st}}$, is approximately 5.6 δ^*_{300} (independent of the streamwise position). Relating the maximum amplitude value of 2.1 δ^*_{300} to this streak distance $\overline{\lambda_{st}}$ reveals a ratio $A_{\max}/\overline{\lambda_{st}} \approx 0.4$. This demonstrates that the breakdown of the instability, accompanied

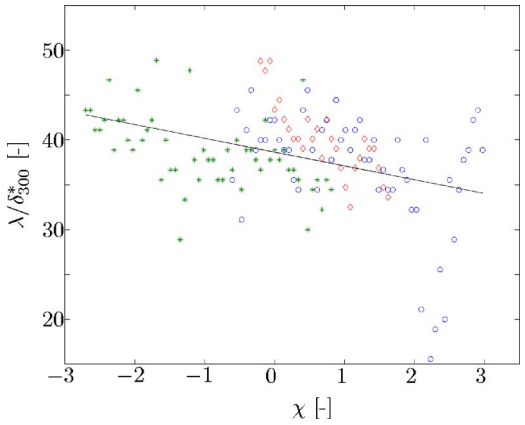

FIG. 3. (Color online) Wavelength as function of χ; the solid line presents a linear fit (symbols are defined in Table I).

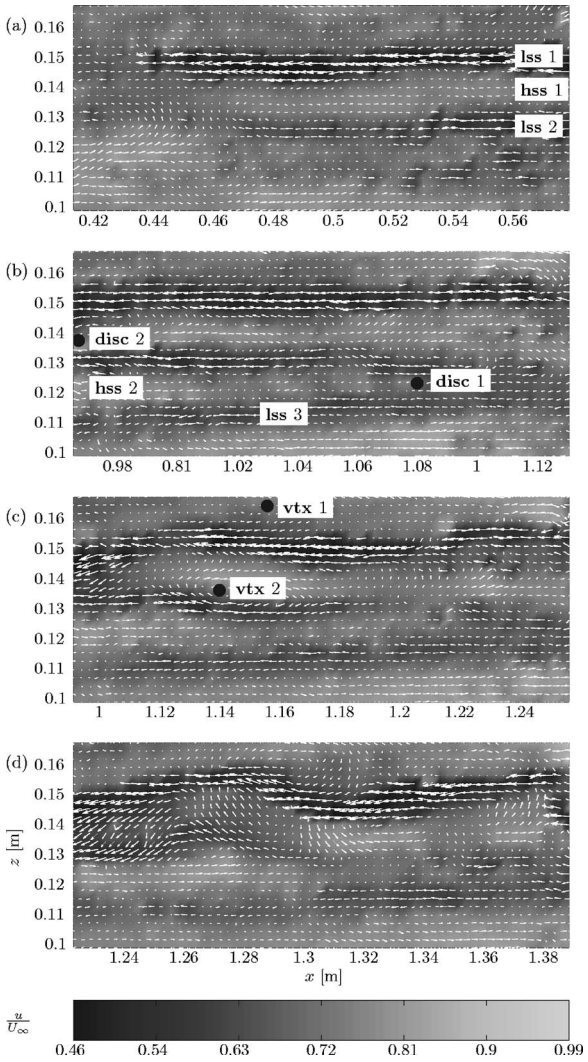

FIG. 4. Evolution in the horizontal plane of three-dimensional structures. Vectors represent the disturbance field (u', w') and the background coloring shows u. The images are taken at $t=-398$, -74, 0, and 77.

by the arising of three-dimensional structures, starts as the oscillation of the unstable low-speed streak exceeds around the centerline of the neighboring high-speed streak. The wavelength of three sinuous instabilities is analyzed (it proved impossible to determine a realistic wavelength for the sinuous instability 4, and instability 3 was already excluded). The development of the wavelength as a function of χ is presented in Fig. 3 (solid lines represent a linear data fit). The wavelength decreases according to a linear trend in the streamwise direction from a value of $\approx 45\delta^*_{300}$ to a value of $\approx 35\delta^*_{300}$.

The characteristic streak configuration and coherent structures developing in the sinuous instability are determined from the development of the instantaneous velocity fields of the five separate instabilities and they are denoted in Fig. 4. Although, as a consequence of the natural breakdown process, each instability still possesses its own specific features. All the images in Fig. 4 originate from the same event, instability 1. The images show a region of $0.165 \times 0.0685\ \text{m}^2$ surrounding the instability and the vectors in the image display the instantaneous disturbance flow

field. The applied background coloring is based on the streamwise dimensionless velocity component, u/U_∞, of the velocity field. Furthermore, the dimensionless time lapses relative to the third image are indicated in the caption. The third image is the first image in which the unstable low speed shows the beginning of the sinuous oscillation, which corresponds to $\mathrm{Re}_{x\mathrm{start}}$ in Table I. Note that the camera traverses with a velocity of $0.72U_\infty$.

The basic streak configuration, which consists of two low-speed streaks (lss1 and lss2) at a small spanwise distance from each other, and a high-speed streak (hss1) in between, is shown in Fig. 4(a). This image shows the velocity field around $x \approx 0.5$ m, $\mathrm{Re}_x = 6.3 \times 10^4$. Structures with a velocity lower than the camera velocity ($0.72U_\infty$) move towards the upstream side of the image, while structures with a larger velocity move downwards. The image reveals that the streaks are not present in the upstream part of the recording domain. In this region the disturbance field still seems to be dominated by the free-stream turbulence eddies. This is due to the wall-normal position of the measuring plane, which is located 5 mm above the wall. Hence, the measuring plane is positioned above the boundary layer in the region close to the leading edge. In Fig. 4(a) half of the measuring plane is apparently located in the boundary layer, while the upstream half is still situated in the free stream.

In Fig. 4(b), the center of the disturbance flow field is located at $x \approx 1.04$ m. The flow field at this point is over the full range perturbed by streaks. The image shows the blockage of the passage of high-speed hss2 at $x \approx 1.07$ m. At this point the low-speed streaks, lss2 and lss3, merge and form one low velocity region. This blockage is referred to as discontinuity 1 (disc1). At the same time, a second discontinuity (disc2) has arisen at the upstream side of the image (just ahead of the picture at $x \approx 0.96$ m). These discontinuities play an important role in the remaining development of the disturbance flow field.

Figure 4(c) displays the disturbance flow field surrounding $x \approx 1.25$ m. This image reveals that both discontinuities (disc1 and disc2) move downstream in the recording area and that two vortices arise in the vicinity of the discontinuities in the flow field, vtx1 and vtx2. The vortices are located in the high shear regions between streaks. The presence of these two vortices is accompanied with a spanwise oscillation of the unstable low-speed streak lss1. The oscillation is antisymmetric with respect to the centerline of the unstable low-speed streak, which demonstrates that it is of the sinuous type. Note that the attendance of discontinuity 1 is somewhat dismantled. The blocked high-speed streak, hss2, has crossed the low-speed streak, lss2, and merges with hss1.

Figure 4(d) shows the flow field around a downstream position of $x \approx 1.31$ m. The image shows regions of high spanwise momentum fluid below the peaks ($x \approx 1.27$ m and $x \approx 1.37$ m), and valley ($x \approx 1.31$ m) of lss1, defined as the last main feature. Vtx1, which was situated between $x \approx 1.26$ m and $x \approx 1.3$ m has disappeared from the disturbance field. The intermediate disturbance fields show that vtx1 is pushed aside by the growing region of high (spanwise) momentum fluid at the left of it. The strength of vtx1 is diminished, while this region expands in the streamwise direction. These high spanwise momentum regions are clearly of a three-dimensional nature and are probably the rollup structures that appear in a sinuous instability just before the final breakdown of the streak. Furthermore, it is relevant to mention that the basic shape of the unstable low-speed streak lss1 remains distinguishable in the flow field for a long distance, despite the intensity increase of the irregular motion with the downstream evolution.

In conclusion, the experimental study reveals that a sinuous secondary instability mode initiates a "natural" breakdown to turbulence in a flat plate boundary layer perturbed with streaks. An analysis of the wave shape shows that the average spanwise and streamwise length scales are, respectively, δ^*_{300} and $40\delta^*_{300}$. It is found that the amplitude increases exponentially in the streamwise direction with a growth rate of approximately 0.01 until a maximum amplitude, $A_{\max} \simeq 2.1\delta^*_{300}$, is reached. At this point the streak starts to fall apart into smaller three-dimensional flow regions. This breakdown process starts as the oscillation of the unstable low-speed streak exceeds about the centerline of the surrounding high-speed streak. The wavelength decreases in the streamwise direction, also according to a linear trend, from a value of more or less $45\delta^*_{300}$ to a value of about $35\delta^*_{300}$. An analysis of the instantaneous disturbance fields reveals the streak configuration and flow interactions during breakdown. First, the sinuous instability arises in a streak configuration with two low-speed streaks located at a small spanwise distance from each other. Second, patches (short streamwise length scale) of low-speed fluid intrude the high-speed streaks surrounding the unstable low-speed streak. Third, in the vicinity of these discontinuities vortices appear in a staggered pattern around the unstable low-speed streak, accompanied by a spanwise oscillation of the unstable streak. The last step is that the vortices develop into three-dimensional flow structures.

[1] S. J. Kline, W. C. Reynolds, F. A. Schraub, and W. P. Runstadler, "The structure of turbulent boundary layer," J. Fluid Mech. **30**, 741 (1967).
[2] P. J. Schmid and D. S. Henningson, *Stability and Transition in Shear Flows* (Springer, New York, 2001).
[3] M. Matsubara and P. H. Alfredsson, "Disturbance growth in boundary layers subjected to free-stream turbulence," J. Fluid Mech. **430**, 149 (2001).
[4] L. Brandt, P. Schlatter P, and D. S. Henningson, "Transition in boundary layers subject to free-stream turbulence," J. Fluid Mech. **517**, 167 (2004).
[5] R. G. Jacobs and P. A. Durbin, "Simulations of bypass transitions," J. Fluid Mech. **428**, 185 (2001).
[6] P. A. Durbin and X. Wu, "Transition beneath vortical disturbances," Annu. Rev. Fluid Mech. **39**, 107 (2007).
[7] W. Schoppa and F. Hussain, "Coherent structure generation in near-wall turbulence," J. Fluid Mech. **453**, 57 (2002).
[8] J. P. J. Hoepffner, L. Brandt, and D. S. Henningson, "Transient growth on boundary layer streaks," J. Fluid Mech. **537**, 91 (2005).
[9] J. Mans, E. C. Kadijk, H. C. de Lange, and A. A. van Steenhoven, "Breakdown in a boundary layer exposed to free-stream turbulence," Exp. Fluids **39**, 1071 (2005).
[10] J. Mans, H. C. de Lange, and A. A. van Steenhoven, "Boundary layer transition process when dealing with free-stream turbulence," in *Turbulence X*, edited by H. I. Andersson and P. A. Krogstad (Trondheim, Norway, 2004), pp. 69–72.
[11] J. Mans, "Streak development and breakdown during bypass transition," Ph.D. thesis, Technische Universiteit Eindhoven, The Netherlands, 2007.
[12] P. Andersson, L. Brandt, A. Bottaro, and D. S. Henningson, "On the breakdown of boundary layers steaks," J. Fluid Mech. **428**, 29 (2001).